

Article

On the Cobalt Content Upgrade in Nickeliferous Laterites Using Iron (III) Sulfate: A Study Based on Thermodynamics Simulations

Rodrigo F. M. Souza ^{1,*}, Mariana A. A. Tavares ¹, Luiz E. C. Cruz ¹, Víctor A. A. Oliveira ², Iranildes D. Santos ³, Francisco J. Moura ¹ and Eduardo A. Brocchi ¹

¹ Department of Chemical and Materials Engineering, Pontifícia Universidade Católica do Rio de Janeiro (PUC-Rio), Rio de Janeiro 22451-900, RJ, Brazil

² Department of Metallurgical and Materials Engineering, Universidade Federal de Ouro Preto (UFOP), Ouro Preto 35400-000, MG, Brazil

³ Instituto Tecnológico Vale (ITV), Ouro Preto 34000-000, MG, Brazil

* Correspondence: rsouza@puc-rio.br; Tel.: +55-21-3527-2379

Abstract: Nickel (Ni) and cobalt (Co) are relevant technological metals for the future of the lithium-ion battery (LIB) industry. Based on the current and projected demand for these, an increased interest in developing processing routes to exploit lateritic occurrences has been observed, as these are reported as critical raw materials for future mineral–metallurgical industry. However, the content of Ni and Co in such ores is minimal and requires impracticable mineral-processing operations for concentration before metal extraction. It was identified that information regarding the sulfation roasting of this material is scarce on what concerns the iron sulfates interaction as a function of the temperature. Based on that context, the present work has its purposes associated with the proposition of an alternative chemical pretreatment to upgrade the content of metals of technological interest in lateritic ores through a simple roast–leach process. Thus, the chemical interactions between the mineral sample and iron (III) sulfate ($\text{Fe}_2(\text{SO}_4)_3$) through thermodynamic simulations and experimental procedures were explored. The latter included specific water leaching practices for the selective concentration of metals. The equilibrium calculations indicate that $\text{Fe}_2(\text{SO}_4)_3$ and FeSO_4 tend to decompose at lower temperatures, and considering the higher stability of other metal sulfates, it could be an interesting reagent in this type of process. Regarding the experimental results, the characterization of materials indicates a recovery of Co as high as 73.4 wt.% after sulfation roasting at 500 °C followed by water leaching, with the full content of Iron (Fe) being reported in the insoluble phase. Based on these findings, the present development could be an interesting alternative to consider within operations for the chemical upgrade of cobalt in such types of mineralogical occurrences.

Keywords: metal sulfates; roast–leach; nickeliferous laterites; cobalt metallurgy



Citation: Souza, R.F.M.; Tavares, M.A.A.; Cruz, L.E.C.; Oliveira, V.A.A.; Santos, I.D.; Moura, F.J.; Brocchi, E.A. On the Cobalt Content Upgrade in Nickeliferous Laterites Using Iron (III) Sulfate: A Study Based on Thermodynamics Simulations. *Minerals* **2022**, *12*, 1156. <https://doi.org/10.3390/min12091156>

Academic Editors: Álvaro Aracena Caipa and Hyunjung Kim

Received: 12 July 2022

Accepted: 8 September 2022

Published: 13 September 2022

Publisher's Note: MDPI stays neutral with regard to jurisdictional claims in published maps and institutional affiliations.



Copyright: © 2022 by the authors. Licensee MDPI, Basel, Switzerland. This article is an open access article distributed under the terms and conditions of the Creative Commons Attribution (CC BY) license (<https://creativecommons.org/licenses/by/4.0/>).

1. Introduction

Nickel (Ni) is very relevant in terms of annual production and, together with iron (Fe), aluminum (Al), manganese (Mn), copper (Cu), zinc (Zn), and lead (Pb), contributes to more than 98 wt.% of all metal industrial production [1]. Moreover, with the current transition to a low-carbon society, an even more expanded importance of these common metals has been expected, as they can provide the required foundations for high-technology applications [2–4]. One of these is related to the development of affordable electrochemical cells to power updated electric transports, in which Ni and cobalt (Co) are important materials for the lithium-ion battery (LIB) industry [5,6]. Co is a typical companion metal in Ni-bearing occurrences, and most of its worldwide production is a byproduct of their extractive metallurgy routes [7,8]. Nevertheless, the consumption and effective allocation of cobalt resources are not balanced at present, thus making it a critical raw material for

the future, which stands as a real challenge to fulfill global demand [9,10]. Therefore, the need for mining expansion without compromising environmental sustainability is obvious, which puts pressure on new technology developments [11].

In terms of Co extraction, the laterite occurrence has been considered a promising source to meet present and future demands [12,13]. This observation seems to be correct, considering that around 70 wt.% of known Ni deposits are related to this type of ore [14–17]. The laterites are in praxis an occurrence formed by the weathering of mafic and ultramafic rocks, typically in warm and rainy regions [18,19], with goethite as the major nickel bearer [20]. Limonite and chlorite could also be observed as important Ni carriers, while Co is typically hosted in oxide crystalline structures [17]. Dealing with the low levels of these metals of interest in such a complex mineralogical matrix is a major challenge in Co extraction, as well as for the Ni itself [21].

Regarding Ni extraction processes, pyrometallurgical operations correspond to a large share of industrial practice [22], with the rotary kiln–electric arc furnace (RKEF) as the dominant technology [23]. Moreover, processes based on acid leaching, pressurized or not, have also been widely reported for laterites [24]. Nevertheless, it is well-described that pure pyro- or hydrometallurgical routes usually deal with high energy and reagent consumption to achieve Ni and Co extraction, inhibiting its application in some of these occurrences. This fact motivates the development of hybrid methods in which the sulfation roast–leach approach appears to be one of the feasible alternatives. The typical sulfation reagents for that method, as reported in the literature, are ammonium sulfate ((NH₄)₂SO₄) [25,26], sulfuric acid (H₂SO₄) [27–29], sodium sulfate (Na₂SO₄) [30,31], sulfur dioxide (SO₂) [32], and trioxide (SO₃) [33]. Research about the use of metal sulfates as laterites sulfation agents is scarce, therefore motivating further developments in this area.

Within this context, the present study deals with the interaction of sulfation roasting using iron (III) sulfate (Fe₂(SO₄)₃) with Co-bearing nickeliferous laterites followed by water leaching to assess the chemical behavior of the reaction system, particularly with respect to Co–Fe separation. The motivation of this work is to provide the first report on the feasibility of the process of a nickeliferous laterite ore reacted in the presence of a metal sulfate. The option of an iron-carrying sulfation reagent is related to the fact that iron (III) and iron (II) sulfates tend to decompose at lower temperatures in comparison to its peers, promoting the formation and stabilization of other sulfates in the system [34,35].

Therefore, the purposes of this work are associated with the development of a detailed and updated thermodynamic assessment of using Fe₂(SO₄)₃ as a sulfation agent based on sulfate formation and stability, as well as an experimental evaluation of some relevant metals' behavior in a simple water-based laterite roast–leach methodology. The study also covers the characterization of materials in the nickeliferous laterite sample, as well as the major reaction products obtained in this study.

2. Materials and Methods

The roasting experiments were carried out using a nickeliferous laterite sample from the northern region of Brazil. The received specifications of the ore mentioned that this sample did not meet the mineralogical site criteria to produce an Fe–Ni alloy based on the high silicate content, and therefore, it would be appropriate to investigate different approaches to increment the grade of some critical metals, such as Ni and Co. Visually, the sample was made up of particles of varying size and predominantly of clay features. To diminish the massive moisture content, typical of lateritic ores, and to avoid interferences of this amount of water in the chemical processing, the sample was dried at 100 °C until a constant mass was achieved and then conditioned in a vacuum. After that, the nickeliferous laterite ore sample was characterized through the methods that are reported in sequence.

2.1. Thermodynamic Simulations

The reaction system equilibrium evaluation was developed using the HSC Chemistry software, version 9.9.2.3 [36]. This part of the study covered the simulations performed

through the Gibbs Energy Minimization method to calculate the resulting equilibrium composition for one independent variable (temperature) and two independent variables (temperature and amount of sulfation reagent).

2.2. Roast–Leach Experiments

After drying, a representative 10 g sample was macerated with iron sulfate III (Isobar) in different concentrations. The mixing proportions were as follows: stoichiometric, 10, 20, and 30 wt.% excess of sulfation reagent. The amount presented here as stoichiometric was based on the reaction of $\text{Fe}_2(\text{SO}_4)_3$ with the detected quantities of Ni and Mg established by the characterization of materials, so that their entire content could react to form their respective sulfates in the case of nickel (NiSO_4) and magnesium (MgSO_4). The Co content was detected below 1 wt.%, and therefore, it was not used for the stoichiometric mass balance. Then, the mixture was transferred to a ceramic crucible where it was submitted to sulfation roasting (SR) at temperatures between 500 and 900 °C inside a muffle furnace (air atmosphere). The purpose of this procedure is to transfer sulfate from $\text{Fe}_2(\text{SO}_4)_3$ to other constituents to form water-soluble salts bearing the cations of interest while Fe reports to oxidized insoluble species. The residence time for the roasting operation was defined as 60 min.

The water leaching (WL) was carried out with distilled water at 80 °C. A volume of 250 mL of solvent in conical flasks along with the roasting product was placed under constant agitation throughout the test. The residence time for this operation was set at 60 min to guarantee full mass transfer of all soluble content. Then, the solid–liquid suspension was subjected to the unitary operation of vacuum filtration to separate the insoluble residue.

Samples of the reaction product from SR as well as the WL insoluble residues were subjected to characterization using the same techniques applied to the nickeliferous laterite ore sample. These methods of characterization are detailed in sequence.

2.3. Materials Characterization

At this stage of the project, the raw material and reaction products were characterized using means of inductively coupled plasma optical spectrometry (ICPOES) via Optima 4300 DV equipment (PerkinElmer), as well as X-ray diffraction through D2 Phaser equipment (Bruker). The former method is related to the quantification of the chemical elements and was prepared through fusion at 80 °C with potassium bisulfate (KHSO_4) due to the high Fe content in the samples. The latter, on the other hand, is associated with quantitative mineralogical analysis [37] through the Rietveld method [38], using the software TOPAS-Academic.

For the iron sulfate characterization and to widen the understanding of its chemical attack over the laterite sample, thermogravimetric analyses (TGA) were performed using STA 449 F3 Jupiter (Netzch) equipment in an inert medium (Linde Gases— N_2 with 99.999% purity) flowing at 20 mL min^{-1} . The experiments were conducted under a heating rate of 10 °C. min^{-1} in the temperature range between 25 and 1200 °C.

3. Results and Discussion

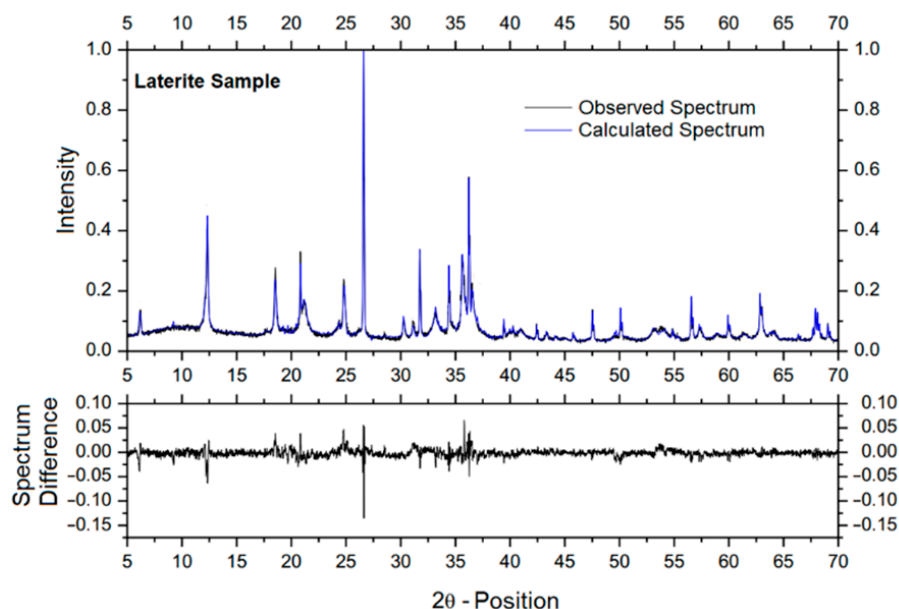
3.1. Laterite Sample Characterization

Table 1 presents the results associated with the major elements of interest within the roast–leach extraction system composing the nickeliferous laterite ore as received. It can be observed that Fe was, by a large margin, the major metallic constituent in the sample, contributing with 30 wt.%. As expected, Si was also a predominant element with 12 wt.%, while the Ni content was 1.7 wt.% of the sample, which is within the typical limits of laterite ores. It is valuable to note that Mg, with 3.1 wt.%, was almost double the nickel mass content. Regarding Co, an amount of 0.07 wt.% was observed. The metallic speciation suggests that the received sample was from an intermediate zone [39].

Table 1. Chemical analysis of the laterite sample using ICPOES.

| Analyzed Metal | Sample Content (wt.%) |
|----------------|-----------------------|
| Ca | 0.06 |
| Co | 0.07 |
| Fe | 30.00 |
| Mg | 3.10 |
| Ni | 1.70 |
| Si | 12.00 |

Figure 1 and Table 2 show the XRD results associated with the laterite sample. The presence of quartz shows that, indeed, the received material could be characterized as silicate laterite (19.5 wt.%). Goethite also appeared in large quantities (32.7 wt.%), confirming a large amount of iron composing it. Combined with hematite (3.4 wt.%) and magnetite (3.7 wt.%), this corroborated the high levels of Fe observed in ICPOES. In addition to these oxidized minerals, 7.3 wt.% of the sample corresponded to a non-specific phase that did not have a defined crystalline structure, following the method described in the literature [40], which may also carry major quantities of iron.

**Figure 1.** XRD mineralogical analysis of the laterite sample: Observed and Calculated Spectra.**Table 2.** XRD mineralogical analysis of the laterite sample: Composition after Rietveld Method calculations.

| Detected Mineral | Sample Content (wt.%) | Detected Mineral | Sample Content (wt.%) |
|------------------|-----------------------|------------------|-----------------------|
| Clinochlore | 3.5 | Magnesiochromite | 3.8 |
| Chlorite | 3.0 | Goethite | 32.7 |
| Lizardite | 12.9 | Halloysite | 4.1 |
| Hematite | 3.4 | Doyleite | 2.1 |
| Magnetite | 3.7 | Birnessite | 2.6 |
| Quartz | 19.5 | Tephroite | 1.4 |

3.2. Thermodynamic Simulations

Based on the hypothesis that $\text{Fe}_2(\text{SO}_4)_3$ could act as an SR reagent, Figure 2 shows the equilibrium composition results as a function of temperature associated with the

stoichiometric chemical interaction between 4/3 mol of this salt and 1 mol of each one of following oxides: nickel (NiO), cobalt (CoO), magnesium (MgO), and calcium (CaO).

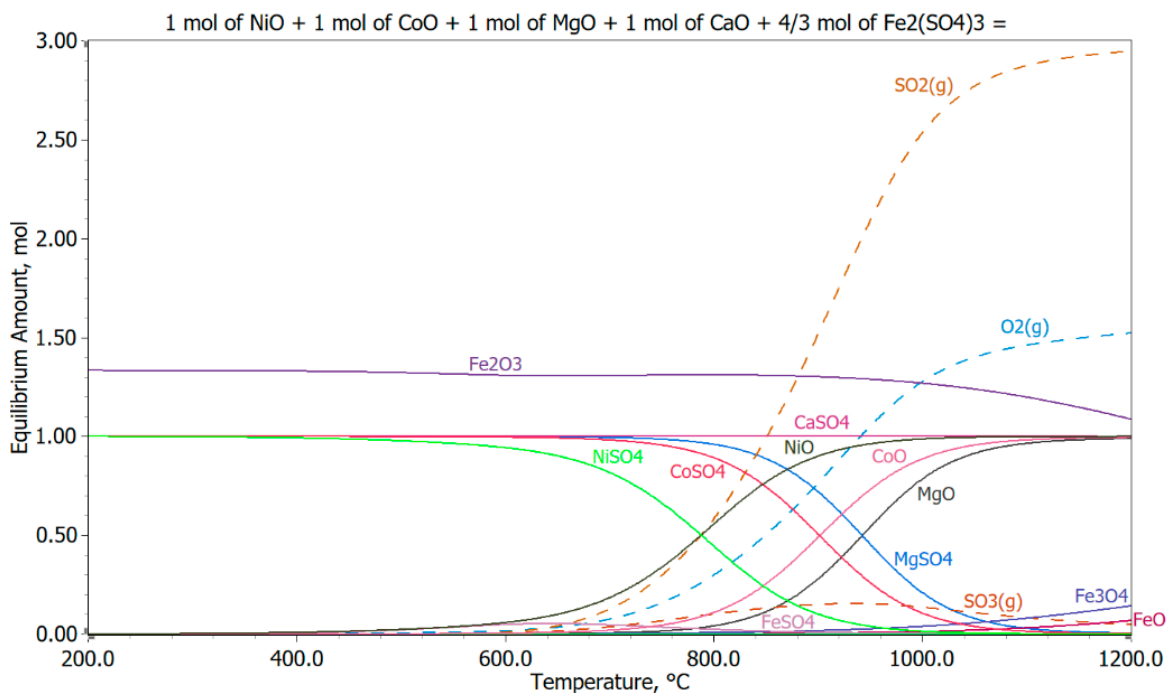


Figure 2. Calculated equilibrium compositions of SR using Fe₂(SO₄)₃ with NiO, CoO, MgO, and CaO at stoichiometric proportions.

Support for the hypothesis comes from the reported fact that iron sulfates tend to decompose at temperatures lower than 700 °C, particularly in the presence of metal with a higher affinity for the sulfate anion [34,35]. Therefore, it could be expected that Fe₂(SO₄)₃ works as a sulfate source to supply Ni, Co, Mg, and Ca with sulfate anions (SO₄²⁻) content. It can be observed that, for the entire temperature range, oxides are the major carriers of iron for selected initial conditions, with negligible FeSO₄ amounts. Fe₂(SO₄)₃, in this context was consumed by the reaction system as predicted and acted as a reagent promoting the sulfation of the oxides of Ni, Co, Mg, and Ca. Concerning sulfate stability, at 584 °C, NiSO₄ remained with 95.0 mol% of its initial composition. A similar behavior was observed for the sulfates of cobalt (CoSO₄) at 755 °C (95.1 mol%) and magnesium at 807 °C (95.2 mol%). Calcium sulfate (CaSO₄), after its formation, was stable in the temperature range. Regarding its selectivity for thermal decomposition, it was verified that NiSO₄ had an equilibrium composition below 1 mol% of the original input in temperatures higher than 1017 °C. The same was observed for CoSO₄ and MgSO₄ at 1117 and 1153 °C, respectively. It is interesting to observe that no prior evolution of SO₂ or SO₃ was relevant for temperatures lower than the one associated with that in which the NiSO₄ thermal decomposition started. This may be considered indicative of sulfate exchange at the selected stoichiometric proportion, which should occur without sulfate loss at low temperatures. Although it is well-known that this was a theoretical simulation with individual oxides, considered as pure species in an ideal mixture, it offers an interesting substrate that there is thermodynamic feasibility of sulfation using this Fe₂(SO₄)₃ as a source of SO₄²⁻. It is also important to mention that one of the premises of this calculation is that the equilibrium composition was reached in a closed system. However, in practice, most sulfation roasting occurs within open systems, particularly concerning the gas flow. Therefore, with the constant removal of the produced SO₂, SO₃, and oxygen (O₂), equilibrium may be shifted, and a decomposition temperature can be reached at even lower values.

Figure 3 presents the equilibrium composition results as a function of the temperature and amount of SR reagent, considering the formation of the respective sulfates based on the chemical attack applied over 1 mol of the following oxides: NiO, CoO, MgO, and CaO.

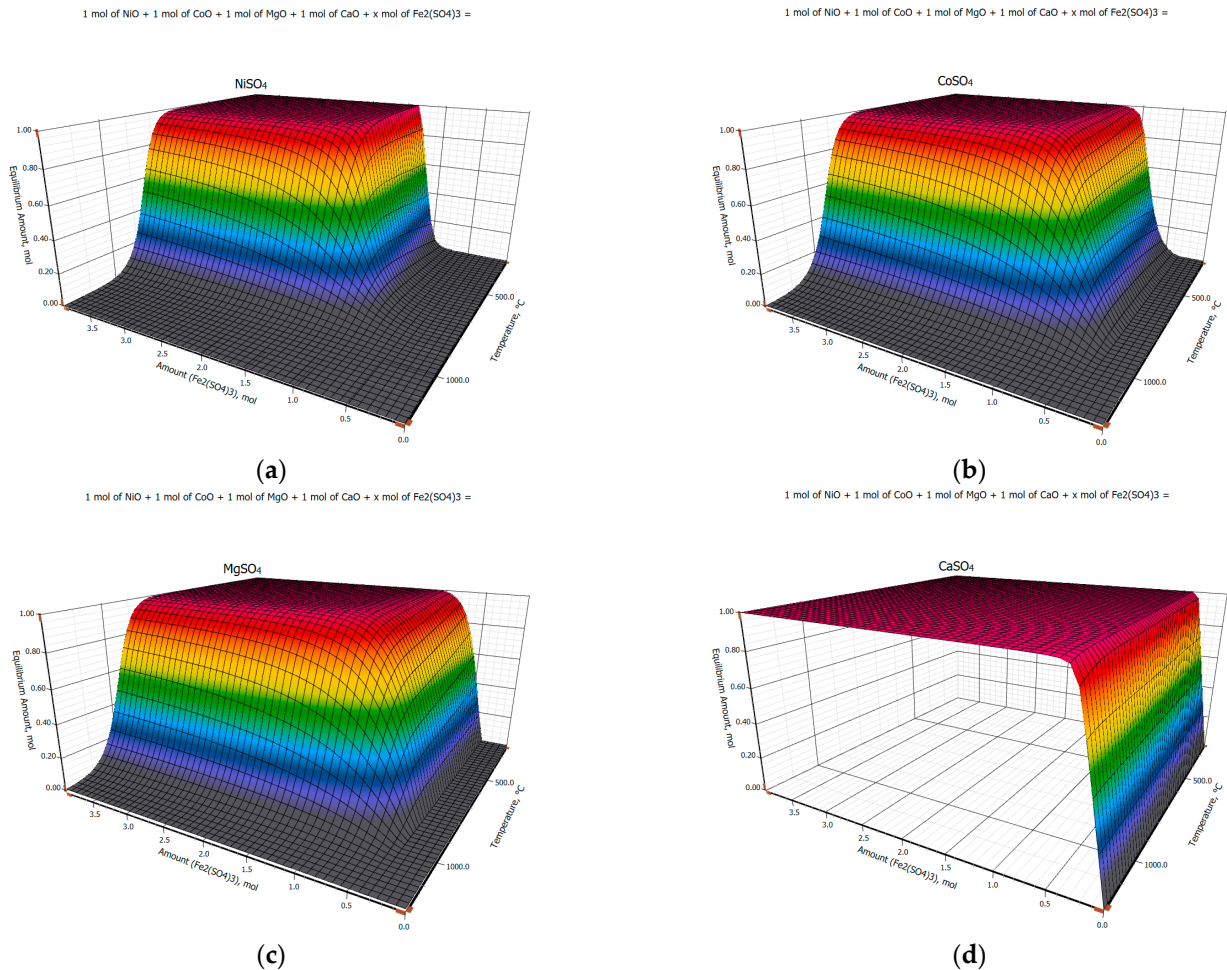


Figure 3. Equilibrium compositions as function of temperature and amount of SR reagent for sulfates formation: (a) NiSO₄; (b) CoSO₄; (c) MgSO₄; (d) CaSO₄.

The results are presented as surfaces of equilibrium for all four associated sulfates that are considered possible products of the sulfation reaction. It is important to mention that these results were obtained after a Gibbs Energy Minimization and provide an optimized picture of the system tendency in a combined manner. As predicted by the Ellingham and predominance diagrams (see Supplementary Material), CaSO₄ had remarkable stability within the limits of the studied variables. This is strongly indicative that this sulfate should be formed preferentially in the SR system. It is also noteworthy that this sulfate was the one that required the smallest amount of Fe₂(SO₄)₃ to form, requiring slightly above 0.3 mol to achieve full sulfation. For MgSO₄, it can be observed that, in terms of Fe₂(SO₄)₃ added to the system, this should be the second formed sulfate, achieving its complete transformation after the system consumed almost 1.0 mol of iron (III) sulfate. Sequentially, CoSO₄ was formed just after 1.1 mol of SR reagent was added, while the same was observed for NiSO₄ with just above 1.3 mol of Fe₂(SO₄)₃ included in the reaction system, following the theoretical stoichiometry proposed in Figure 2. These tendencies could be valuable information for defining the sulfation mechanism, which is currently not under the scope of the manuscript but should be appreciated in future works.

Nevertheless, it is possible to affirm that a sulfation roasting system could be calibrated, theoretically, for salt formation and consequent separation using leaching followed by

filtration. Regarding the thermal decomposition of the formed sulfates, it can be observed for Ni, Co, and Mg that increments of $\text{Fe}_2(\text{SO}_4)_3$ slightly increased the stability of the formed sulfates based on the temperature at which this process started.

3.3. Roast–Leach Experiments

For the present study in which the reagent proportion and the temperature effect were first appreciated, the procedure of SR was carried out for a fixed reaction time of 30 min inside a muffle furnace, plus 5 min for thermal stabilization. Based on the thermodynamic simulations and the TGA results of the $\text{Fe}_2(\text{SO}_4)_3$ (see Supplementary Material), the temperatures at which SR was conducted were defined as between 500 and 900 °C. This range was selected to promote the full decomposition of iron sulfate and the consequent offer of SO_4^{2-} to other cations within the mineralogical matrix of the laterite sample. In this context, Figure 4 shows the mass variation results for SR and WL operations for the following conditions: stoichiometric, 10, 20, and 30 wt.% excess of sulfation reagent.

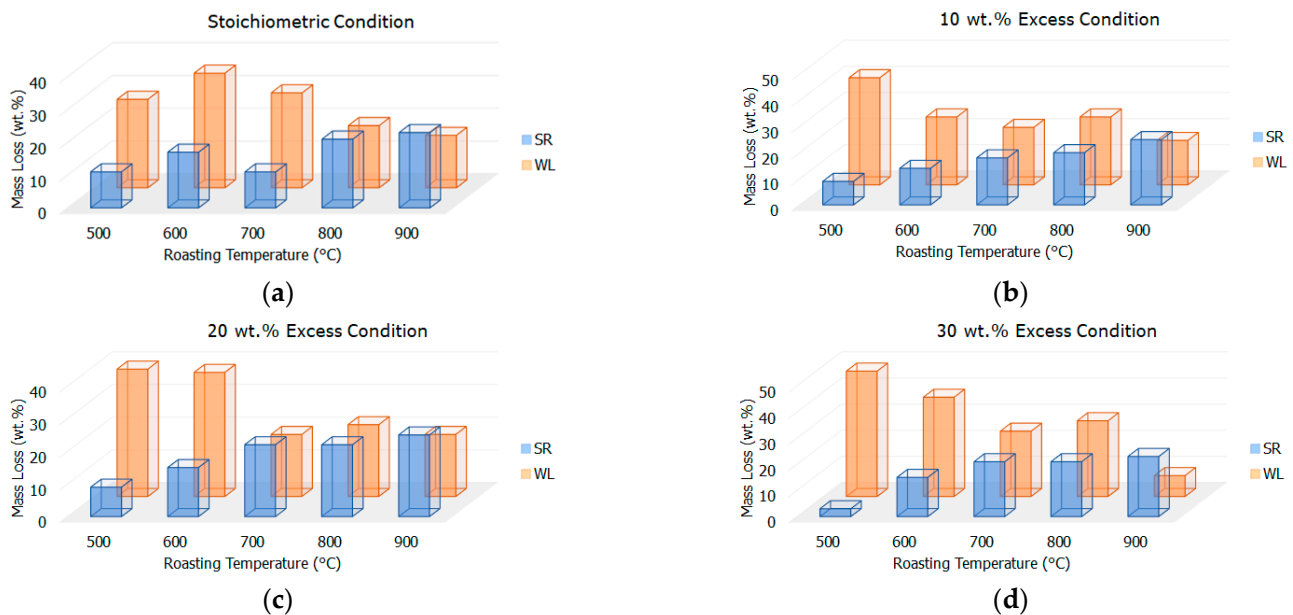


Figure 4. SR and WL mass variation results: (a) at Stoichiometric Condition; (b) at 10 wt.% Excess Condition; (c) at 20 wt.% Excess Condition; (d) at 30 wt.% Excess Condition.

For the stoichiometric condition, higher levels of solubilized material at 500, 600, and 700 °C can be observed. The mass loss levels in roasting were approximately constant, with more prominent variation at 800 and 900 °C. Based on these observations, it can be noticed that this behavior is most probably related to the thermal decomposition of the sulfation system reagent as well as the desulfation of the formed sulfates. Regarding the conditions of excess, it can be verified that SR mass loss seemed to behave progressively until it reached a plateau of maximum as the temperature increased, while for WL, the opposite can be noticed, with a decrescent variation. It is noteworthy that, at 30 wt.% excess, the maximum levels of solubilized material were achieved, suggesting that $\text{Fe}_2(\text{SO}_4)_3$ was decomposing and offering sulfate to minerals in the laterite sample, forming leachable species.

Based on the motivation to verify the feasibility of the process, this condition was chosen for further characterization of materials using TGA, as shown in Figure 5.

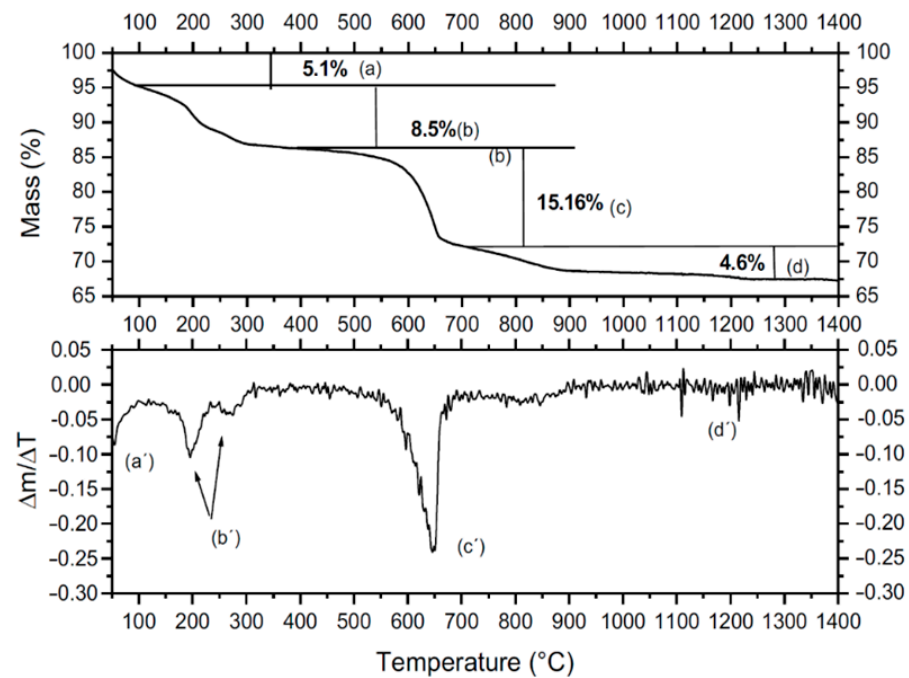


Figure 5. TGA and DTG behavior of the sample with 30 wt.% excess of $\text{Fe}_2(\text{SO}_4)_3$ as SR reagent.

It can be observed that event (a) represents the loss of residual water adsorbed by the ore that has not been eliminated on drying. Sequentially, in event (b), there is a loss of water from iron sulfate III and the thermal decomposition of goethite [17]. For 30 wt.% excess of iron sulfate III, the expected mass loss would be 5.2 wt.% of mass loss due to sulfate decomposition and 2.8 wt.% related to the thermal decomposition of goethite. The total mass loss would be 8 wt.%, which is, in fact, close to the one observed. In event (c), on the other hand, there is a thermal decomposition of the chlorites and also mass loss related to $\text{Fe}_2(\text{SO}_4)_3$. According to the thermodynamic study, it is believed that this loss could be related to the partial decomposition of some sulfates present in the reaction system. Based on the reported literature, the sulfates of Mg and Ca are not supposed to decompose at event (c) [41,42]. The last event with the lowest mass loss reported tends to be associated with talc decomposition [17,43] as well as MgSO_4 transformation into MgO [41,44].

3.4. Reaction Products Characterization

Table 3 presents the results related to the recovery of major elements of interest in the solution recovered from WL following the SR process at 500 and 700 °C, with the condition of 30 wt.% excess of $\text{Fe}_2(\text{SO}_4)_3$.

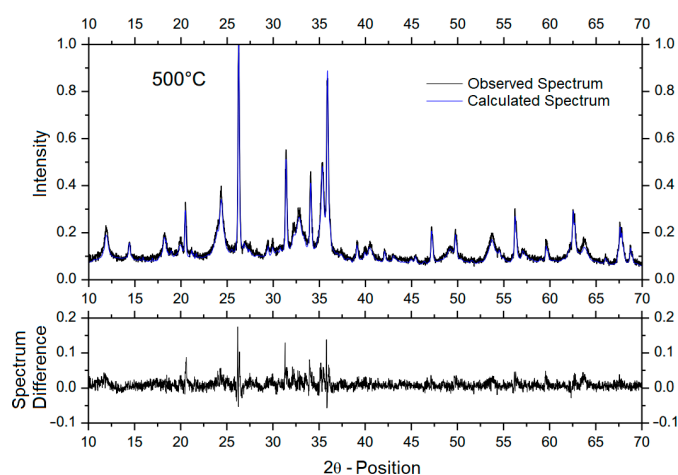
Table 3. Chemical analysis of the WL solutions in terms of sample recovery using ICPOES.

| Analyzed Metal | WL 500 °C Sample Recovery (wt. %) | WL 700 °C Sample Recovery (wt. %) |
|----------------|-----------------------------------|-----------------------------------|
| Ca | 31.1 | 29.6 |
| Co | 73.4 | 67.6 |
| Fe | 4.2 | 0.5 |
| Mg | 23 | 57.9 |
| Ni | 28.7 | 33.7 |
| Si | 2.3 | 1.6 |

It can be observed that the levels of Fe content are low in all three campaigns, indicating that iron (III) sulfate offers, based on chemical affinity or thermal decomposition, its anion to other constituents in the mixture. After 600 °C, it is expected that Fe reports solely to the insoluble phase [35]. It is interesting to note that Co recovery levels were higher than

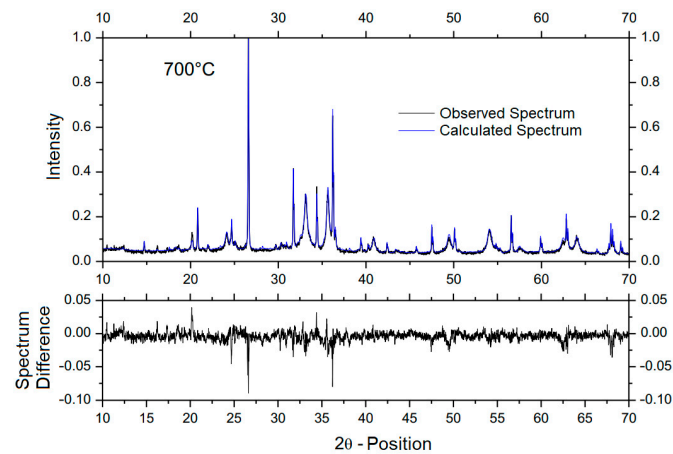
any other element, even compared to Ca and Mg, which based on the thermodynamics assessment for pure oxides, have a theoretical preference for sulfation. However, in a more stable mineralogical structure, Ca and Mg may not form sulfates and may remain associated with their original silicates. As Co and Ni are primarily substitutional elements in laterite minerals, it could be possible that the sulfation chemical attack is more active over them. However, the recovery levels for the Ni were low, ranging from 23 to 34 wt.%, indicating that the sulfate decomposition had already taken place or inefficient sulfation roasting for this element. One possibility for the latter is the evolution of SO_2 and SO_3 from $\text{Fe}_2(\text{SO}_4)_3$ decomposition, restricting the contact of Ni with sulfur-bearing species. This could be the object of future research considering SR using iron (III) sulfate decomposition. Still, the Co concentration combined with the almost full removal of Fe and Si from the recovered liquors indicates that such a route can be a promising alternative for chemical beneficiation of silicate laterite ores, regarding the partial concentration of this element. For Ni, however, further studies should be developed.

Finally, Figures 6 and 7 as well as Table 4 show the XRD results related to the roast–leach products after SR at 500 and 700 °C with the condition of 30 wt.% excess of $\text{Fe}_2(\text{SO}_4)_3$. It is noteworthy that iron sulfates were present in a minor quantity in SR samples, suggesting that operational conditions could be further enhanced. Most importantly, however, the quantity of iron oxides under three conditions, both for SR and WL samples, indicated high levels of decomposition. It is important to note that most of the insoluble WL residues were, as expected, composed of Fe and Si oxides, combining for more than 70 wt.% of the sample. This fact confirms the premise that silicate laterite ores can be chemically beneficiated using an SR based on $\text{Fe}_2(\text{SO}_4)_3$, as this content primarily reports to the insoluble phase, with a partial concentration of Ni and Co in the solution. Future studies will deepen this development by focusing on obtaining high recovery levels. It is important to mention that some losses of Ni and Co have been reported in processes of sulfation followed by water leaching, mostly carried by hematite [29]. Nevertheless, considering the low levels of Co within the starting material, the reported results are motivating as they could provide some relevant degree of concentration with the concomitant separation of Fe and Si.



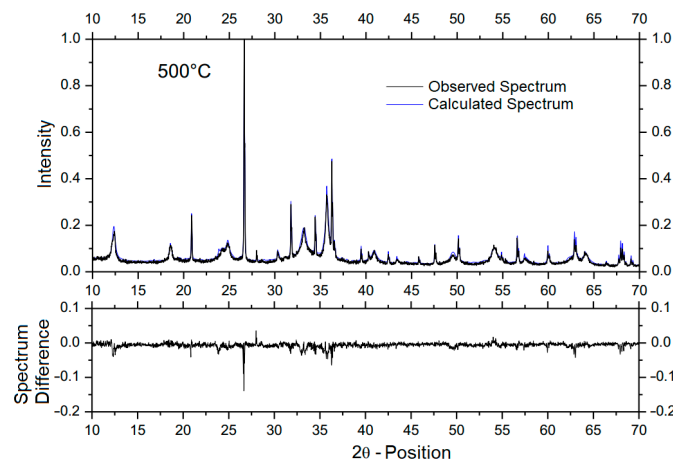
(a)

Figure 6. Cont.

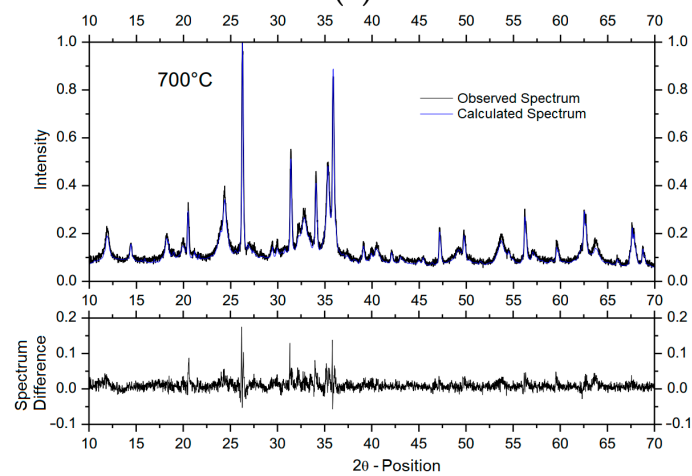


(b)

Figure 6. XRD mineralogical analysis of the roasted material: Observed and Calculated Spectra for the samples processed at (a) 500 °C and (b) 700 °C.



(a)



(b)

Figure 7. XRD mineralogical analysis of the insoluble material after leaching followed by filtration: Observed and Calculated Spectra for the samples processed at (a) 500 °C and (b) 700 °C.

Table 4. XRD mineralogical analysis of the roasted material as well as the insoluble material after leaching followed by filtration: Composition after Rietveld Method calculations.

| Detected Mineral | SR 500 °C Sample Recovery (wt.%) | WL 500 °C Sample Recovery (wt.%) | SR 700 °C Sample Recovery (wt.%) | WL 700 °C Sample Recovery (wt.%) |
|---|----------------------------------|----------------------------------|----------------------------------|----------------------------------|
| Hematite | 21.02 | 47.5 | 33.01 | 44.84 |
| Magnetite | 2.75 | 4.70 | 2.33 | 3.01 |
| Quartz | 15.2 | 27.8 | 20.15 | 24.97 |
| Magnesiochromite | - | 1.38 | 0.13 | 0.16 |
| Chromite | 1.33 | 0.44 | 0.60 | 0.43 |
| Clinocllore | 2.49 | 2.90 | 1.38 | 10.69 |
| Melanterite | 2.75 | 4.31 | - | 4.40 |
| Na _{7.5} Al ₆ Si ₆ O ₂₄ S _{4.5} | 4.73 | 5.90 | 1.44 | 0.64 |
| Halloysite | 2.53 | 1.90 | 3.12 | - |
| Lepidocrocite | 1.36 | - | 0.37 | - |
| Fe ₂ (SO ₄) ₃ ·3H ₂ O | 0.87 | - | 1.56 | - |
| Fe ₂ (SO ₄) ₃ ·FeSO ₄ ·2H ₂ O | 2.03 | - | 3.01 | - |
| Lizardite | 1.74 | - | - | - |

4. Final Remarks

Chemical beneficiation of nickeliferous laterite ore based on iron sulfate roasting was proposed based on an updated thermodynamic assessment. Based on the thermodynamic simulations, it was verified that Fe₂(SO₄)₃, as it decomposes at lower temperatures, can be used as a source of sulfate in roasting systems. It was also observed that CoSO₄ tends to decompose at a higher temperature, therefore suggesting a higher stability in comparison to NiSO₄. On the other hand, for MgSO₄ and CaSO₄, it was observed that, after formation, these salts tend to be highly stable.

The experimental results indicate that Mg and Ca sulfates have higher stability within their mineralogical phases and, therefore, a poor chemical attack during the iron sulfate roasting. Regarding Ni and Co, it was observed that the former has a recovery level at the processing temperatures explored in this study between 23.8 and 33.7 wt.%, suggesting a possible decomposition after formation, while the latter has recovery as high as 70 wt.% after roasting at 500 °C and water leaching. Therefore, considering that Co content in the received sample was below 1 wt.%, this scenario suggests a promising alternative for chemical beneficiation of Ni–Co content. Further studies can be developed to increase both recoveries.

Supplementary Materials: The following supporting information can be downloaded at: <https://www.mdpi.com/article/10.3390/min12091156/s1>. Figure S1: Ellingham diagram for sulfates formation based on a fixed quantity of O₂; Figure S2: Predominance diagrams as function of temperature for a fixed quantity of oxygen (0.21 bar): (a) S-Fe-O system; (b) S-Ni-O system; (c) S-Co-O system; (d) S-Mg-O system; (e) S-Ca-O system; Figure S3: TGA and DTG characterization of the sample as received; Figure S4: TGA characterization of the iron sulfate used as sulfation roasting reagent.

Author Contributions: Conceptualization, V.A.A.O. and R.F.M.S.; methodology, M.A.A.T., V.A.A.O. and R.F.M.S.; software, V.A.A.O. and R.F.M.S.; validation, V.A.A.O. and R.F.M.S.; formal analysis, M.A.A.T., L.E.C.C., V.A.A.O., F.J.M. and R.F.M.S.; investigation, R.F.M.S., I.D.S. and V.A.A.O.; resources, R.F.M.S., I.D.S., V.A.A.O., F.J.M. and E.A.B.; data curation, M.A.A.T. and R.F.M.S.; writing—original draft preparation, R.F.M.S., M.A.A.T. and L.E.C.C.; writing—review and editing, I.D.S., V.A.A.O., F.J.M. and E.A.B.; visualization, L.E.C.C. and R.F.M.S.; supervision, V.A.A.O. and R.F.M.S.; project administration, I.D.S. and R.F.M.S.; funding acquisition, E.A.B. and R.F.M.S. All authors have read and agreed to the published version of the manuscript.

Funding: This study was financed in part by the Coordenação de Aperfeiçoamento de Pessoal de Nível Superior—Brasil (CAPES)—Finance Code 001.

Institutional Review Board Statement: Not applicable.

Informed Consent Statement: Not applicable.

Data Availability Statement: Not applicable.

Acknowledgments: The authors acknowledge their gratitude to the Instituto Tecnológico Vale/Vale S.A. for technical support. The institute contribution was essential for the consolidation of a research initiative for future developments related to silicate nickeliferous laterites and the treatment of its possible byproducts. The authors are also grateful to the Vice-Reitoria para Assuntos Acadêmicos da Pontifícia Universidade Católica do Rio de Janeiro (VRAC/PUC_Rio), the Fundação Carlos Chagas Filho de Amparo à Pesquisa do Estado do Rio de Janeiro (FAPERJ), as well as the Conselho Nacional de Desenvolvimento Científico e Tecnológico (CNPq) for the partnership and financial support throughout the research.

Conflicts of Interest: The authors declare that they have no known competing financial interest or personal relationship that could have appeared to influence the work reported in this paper.

References

1. Elshkaki, A.; Graedel, T.E.; Ciacci, L.; Reck, B.K. Resource Demand Scenarios for the Major Metals. *Environ. Sci. Technol.* **2018**, *52*, 2491–2497. [[CrossRef](#)] [[PubMed](#)]
2. Nakajima, K.; Daigo, I.; Nansai, K.; Matsubae, K.; Takayanagi, W.; Tomita, M.; Matsuno, Y. Global distribution of material consumption: Nickel, copper, and iron. *Resour. Conserv. Recycl.* **2018**, *133*, 369–374. [[CrossRef](#)]
3. Aznar-Sánchez, J.A.; Velasco-Muñoz, J.F.; García-Gómez, J.J.; López-Serrano, M.J. The Sustainable Management of Metals: An Analysis of Global Research. *Metals* **2018**, *8*, 805. [[CrossRef](#)]
4. Watari, T.; McLellan, B.C.; Giurco, D.; Dominish, E.; Yamasue, E.; Nansai, K. Total material requirement for the global energy transition to 2050: A focus on transport and electricity. *Resour. Conserv. Recycl.* **2019**, *148*, 91–103. [[CrossRef](#)]
5. Weimer, L.; Braun, T.; vom Hemdt, A. Design of a systematic value chain for lithium-ion batteries from the raw material perspective. *Resour. Policy* **2019**, *64*, 101473. [[CrossRef](#)]
6. Turcheniuk, K.; Bondarev, D.; Amatucci, G.G.; Yushin, G. Battery materials for low-cost electric transportation. *Mater. Today* **2020**, *42*, 57–72. [[CrossRef](#)]
7. Graedel, T.E. Grand Challenges in Metal Life Cycles. *Nat. Resour. Res.* **2018**, *27*, 181–190. [[CrossRef](#)]
8. Dehaine, Q.; Tijsseling, L.T.; Glass, H.J.; Törmänen, T.; Butcher, A.R. Geometallurgy of cobalt ores: A review. *Miner. Eng.* **2021**, *160*, 106656. [[CrossRef](#)]
9. Mudd, G.M.; Jowitt, S.M. Global Resource Assessments of Primary Metals: An Optimistic Reality Check. *Nat. Resour. Res.* **2018**, *27*, 229–240. [[CrossRef](#)]
10. Dong, X.; An, F.; Dong, Z.; Whang, Z.; Jiangm, M.; Yang, P.; An, H. Optimization of the international nickel ore trade network. *Resour. Policy* **2021**, *70*, 101978. [[CrossRef](#)]
11. Aznar-Sánchez, J.A.; Velasco-Muñoz, J.F.; Belmonte-Ureña, L.J.; Manzano-Agugliaro, F. Innovation and technology for sustainable mining activity: A worldwide research assessment. *J. Clean. Prod.* **2019**, *221*, 38–54. [[CrossRef](#)]
12. Mudd, G.M. Global trends and environmental issues in nickel mining: Sulfides versus laterites. *Ore Geol. Rev.* **2010**, *38*, 9–26. [[CrossRef](#)]
13. Elitok, Ö.; Tavlan, M. Geology and economic potential of Ni deposits. *Mod. Approaches Solid Earth Sci.* **2019**, *16*, 635–653. [[CrossRef](#)]
14. Kaya, S.; Topkaya, Y.A. High pressure acid leaching of a refractory lateritic nickel ore. *Miner. Eng.* **2011**, *24*, 1188–1197. [[CrossRef](#)]
15. Norgate, T.; Jahanshahi, S. Assessing the energy and greenhouse gas footprints of nickel laterite processing. *Miner. Eng.* **2011**, *24*, 698–707. [[CrossRef](#)]
16. Ma, B.; Yang, W.; Pei, Y.; Wang, C.; Jin, B. Effect of activation pretreatment of limonitic laterite ores using sodium fluoride and sulfuric acid on water leaching of nickel and cobalt. *Hydrometallurgy* **2017**, *169*, 411–417. [[CrossRef](#)]
17. Oliveira, V.A.; Santos, C.G.; Brocchi, E.A. Assessing the Influence of NaCl on the Reduction of a Siliceous Laterite Nickel Ore Under Caron Process Conditions. *Metall. Mater. Trans. B* **2019**, *50*, 1309–1321. [[CrossRef](#)]
18. Butt, C.R.M.; Cluzel, D. Nickel Laterite Ore Deposits: Weathered Serpentinites. *Elements* **2013**, *9*, 123–128. [[CrossRef](#)]
19. Tupaz, C.A.; Watanabe, Y.; Sanematsu, K.; Echigo, T. Mineralogy and geochemistry of the Berong Ni-Co laterite deposit, Palawan, Philippines. *Ore Geol. Rev.* **2020**, *125*, 103686. [[CrossRef](#)]
20. Basturku, H.; Acarkan, N.; Gock, E. The role of mechanical activation on atmospheric leaching of a lateritic nickel ore. *Int. J. Miner. Proc.* **2017**, *163*, 1–8. [[CrossRef](#)]
21. Quast, K.; Connor, J.N.; Skinner, W.; Robinson, D.J.; Addai-Mensah, J. Preconcentration strategies in the processing of nickel laterite ores, Part 1: Literature review. *Miner. Eng.* **2015**, *79*, 261–268. [[CrossRef](#)]
22. Stankovic, S.; Stopic, S.; Sokic, M.; Markovic, B.; Friedrich, B. Review of the Past, Present, and Future of the Hydrometallurgical Production of Nickel and Cobalt from Lateritic Ores. *Metall. Mater. Eng.* **2020**, *26*, 199–208. [[CrossRef](#)]
23. Keskinilic, E. Nickel Laterite Smelting Processes and Some Examples of Recent Possible Modifications to the Conventional Route. *Metals* **2019**, *9*, 974. [[CrossRef](#)]
24. Meshram, P.; Abhilash; Pandey, B.P. Advanced Review on Extraction of Nickel from Primary and Secondary Sources. *Miner. Proc. Extr. Metall. Rev.* **2019**, *40*, 157–193. [[CrossRef](#)]

25. Li, J.; Chen, Z.; Shen, B.; Xu, Z.; Zhanf, Y. The extraction of valuable metals and phase transformation and formation mechanism in roasting–water leaching process of laterite with ammonium sulfate. *J. Clean. Prod.* **2017**, *140*, 1148–1155. [[CrossRef](#)]
26. Li, J.; Li, Y.; Duan, H.; Guo, X.; Zhai, Y. Experimental and Kinetic Study of Magnesium Extraction and Leaching from Laterite Nickel Ore by Roasting with Ammonium Sulfate. *Rus. J. Non-Ferrous Metal* **2018**, *59*, 596–604. [[CrossRef](#)]
27. Li, D.; Parl, K.H.; Wu, Z.; Guo, X.Y. Response surface design for nickel recovery from laterite by sulfation–roasting–leaching process. *Trans. Nonferrous Metals Soc. China* **2010**, *20*, s92–s96. [[CrossRef](#)]
28. Parlak, T.T.; Yildiz, K. Effects of Sulfation Roasting and Sodium Sulfate Addition on Dissolution of Nickel and Cobalt from Laterite. *Acta Phys. Pol. A* **2017**, *136*, 629–631. [[CrossRef](#)]
29. Ribeiro, P.P.M.; Souza, L.C.M.; Neumann, R.; Santos, I.D.; Dutra, A.J.B. Nickel and cobalt losses from laterite ore after the sul-fation–roasting–leaching processing. *J. Mater. Res. Technol.* **2020**, *9*, 12404–12415. [[CrossRef](#)]
30. Guo, X.Y.; Li, D.; Park, K.H.; Tian, Q.H.; Wu, Z. Leaching behavior of metals from a limonitic nickel laterite using a sulfation roasting–leaching process. *Hydrometallurgy* **2009**, *99*, 144–150. [[CrossRef](#)]
31. Samadhi, T.J. Thermochemical analysis of laterite ore alkali roasting: Comparison of sodium carbonate, sodium sulfate, and sodium hydroxide. *AIP Conf. Proc.* **2017**, *1805*, 040008. [[CrossRef](#)]
32. Papazoglou, D.; Rankin, W.J. Direct sulfation of nickel laterite ores using sulfur dioxide rich gases. In *Yazawa International Symposium on Metallurgical and Materials Processing*; Wiley: San Diego, CA, USA, 2–6 March 2003; Volume 1, pp. 755–769.
33. Bainbridge, D.W. Sulfation of a nickeliferous laterite. *Metall. Trans.* **1973**, *4*, 1655–1658. [[CrossRef](#)]
34. Prasad, S.; Pandey, B.D. Sulphation roasting studies on synthetic copper–iron sulphides with steam and oxygen. *Can. Metall. Q.* **1999**, *38*, 237–247. [[CrossRef](#)]
35. Souza, R.; Queiróz, C.; Brant, J.; Brocchi, E. Pyrometallurgical processing of a low copper content concentrate based on a thermodynamic assessment. *Miner. Eng.* **2019**, *130*, 156–164. [[CrossRef](#)]
36. Roine, A. *HSC Chemistry*; Metso Outotec: Pori, Finland, 2018.
37. Cheary, R.W.; Coelho, A. A fundamental parameters approach to X-ray line-profile fitting. *J. Appl. Crystallogr.* **1992**, *25*, 109–121. [[CrossRef](#)]
38. Coelho, A.A. *TOPAS-Academic*; TOPAS-Academic: Brisbane, Australia, 2007.
39. Burkin, A.R. Extractive Metallurgy of Nickel. In *Critical Reports on Applied Chemistry*; Wiley–Blackwell: Hoboken, NJ, USA, 1987; p. 160, ISBN 463 13:978-0471914259.
40. Basturku, H.; Acarkan, N. Separation of nickel and iron from lateritic ore using a digestion–roasting–leaching–precipitation process. *Physicochem. Prob. Miner. Proc.* **2016**, *52*, 564–574. [[CrossRef](#)]
41. Scheidema, M.N.; Taskinen, P. Decomposition Thermodynamics of Magnesium Sulfate. *Ind. Eng. Chem. Res.* **2011**, *50*, 9550–9556. [[CrossRef](#)]
42. Yan, Z.; Wang, Z.; Wang, X.; Liu, H.; Qiu, J. Kinetic model for calcium sulfate decomposition at high temperature. *Trans. Nonferrous Metals Soc. China* **2015**, *25*, 3490–3497. [[CrossRef](#)]
43. Duglogorski, B.Z.; Balucan, R.D. Dehydroxylation of serpentine minerals: Implications for mineral carbonation. *Renew. Sustain. Energy Rev.* **2014**, *31*, 353–367. [[CrossRef](#)]
44. Souza, B.; Souza, R.; Santos, I.; Brocchi, E. MgSO₄ carbothermic reductive decomposition to produce a highly reactive MgO powder. *J. Mater. Res. Technol.* **2020**, *9*, 1847–1855. [[CrossRef](#)]